POTENTIAL OF NON - AZEOTROPIC REFRIGERANT MIXTURE AS WORKING REFRIGERANT IN HOT WATER HEAT PUMPS

FJ Smit and JP Meyer

Research Group for Heating and Cooling Technology, Laboratory for Energy, PO Box 524, Auckland Park, 2006, South Africa, Fax:27 11 489 2466,
E-mail:jpm@ing1.rau.ac.za
(Please address all correspondence to second author)

Abstract

Industry is only using 20% of the heat subtracted from fossil fuels. The other 80% is released to the surroundings leading to an increase in the global warming effect.

In contrast to this, the output of a heat pump is always more than the input, it delivers up to 67% energy savings, has less pollution than conventional heating methods and has a smaller influence on the greenhouse effect because it delivers less carbon dioxide to the atmosphere than other heating methods.

The performance of a heat pump is influenced by the properties of the refrigerant that is used. The refrigerant that is mostly used in hot water heat pumps is R22. It supplies hot water at temperatures of 60 to 65 °C.

In this study it is theoretically shown that a non - azeotropic refrigerant mixture of R22 and R142b has the potential to increase the COP, reduce the pressure ratio of the compressor, maintain chemical stability of refrigerant and lubrication oil, increase heating capacity and display the feature of varying the heating capacity with load.

The main aim of this study is to design and evaluate a hot water heat pump that uses a non - azeotropic refrigerant mixture, so that the potential of a non - azeotropic refrigerant mixture may be determined.

1. NOMENCLATURE

COP	coefficient of performance
C_p	specific heat at constant pressure
d_i	inside diameter of inner pipe of the pipe-in-pipe heat exchanger
d_o	outside diameter of inner pipe of the pipe-in-pipe heat exchanger
h	enthalpy
h_r	refrigerant heat transfer coefficient
h_w	water heat transfer coefficient
k	thermal conductivity
L_{io}	length of region between inlet and outlet
m	refrigerant mass flow
m_w	water mass flow
P	compressor input power
Q_{io}	heat rejected (absorbed) by the refrigerant or water in a region
T_{io}	region logarithmic mean temperature difference between inlet and outlet
U_{io}	region overall heat transfer coefficient between inlet and outlet
V	displacement rate
η	efficiency
ρ	density

Subscripts

1 to 7	different stations in Figure 1
i	inlet
m	mixture
o	outlet
r	pure refrigerant (i.e. R22)
s	isentropic
v	volumetric
w	water

2. INTRODUCTION

With the current increase in the use of coal, South Africa's main resources will be exhausted within the next 90 years (Johannsen and Kaiser 1986). Industry uses only 20% (Walker 1993) of the heat that is extracted from fossil fuels, the other 80% is delivered to the surroundings and leads to the increase in the global warming effect (Salas and Mariane 1992). Fossil fuels are further more used in industry to heat water. In domestic applications an electrical geyser is used for water heating. In Bassons (1983) study, he mentioned that 50% of all South African electricity used for domestic applications is used for the heating of water.

Hot water heat pumps are a more suitable method of heating water and have been used for some time. It delivers up to 67% energy savings in domestic applications (Meyer and Greyvenstein 1992), delivers less pollution than conventional methods of heating and has a smaller contribution to the green house effect because it delivers less carbon dioxide into the atmosphere than other heating methods. Furthermore the output of a heat pump is always more than the input.

The performance of a heat pump can be increased if the COP of the heat pump is increased. An increase in COP means that the same amount of heating can be done with less compressor power. A reduction in compressor power can be obtained if a non - azeotropic refrigerant mixture is used (Johannsen 1992).

A non - azeotropic refrigerant mixture is a mixture of refrigerants that undergo non - isothermal (sliding temperature, also called temperature glides) phase changes with a change in concentration, at constant pressure.

Johannsen (1992) investigated theoretically the use of a wide range of non - azeotropic refrigerant mixtures in water heating heat pumps under South African conditions. He selected a mixture of R22 and R142b, which is environmentally acceptable, commercially available and fully compatible with materials and lubricants used in current heat pump designs.

It is the purpose of this study to investigate the behaviour of different concentrations of the mixture of R22 and R142b in hot water heat pumps. To make this possible detailed heat pump design methodologies have to be developed that may be used to predict the performances. Although the performances can be calculated by developing a computer programme, hand calculations will be used in this study to develop a better grasp of the interaction of the refrigerant variables used. In order to simplify the design, the heat pump system selected is a water-to-water heat pump with counter flow pipe-in-pipe heat exchangers, with the refrigerant on the inner and the water on the outer annulus. It is not the aim of this study to optimise the system. This may be done at a later stage, preferably after the development of a computer programme, and after positive results from this study.

The outline of this paper is as follows: Firstly the design methodologies of a pure R22 heat pump is discussed, there after, the design methodology of a non - azeotropic refrigerant mixture heat pump are considered for different concentrations of R22 and R142b. The method used to compare the performance of the heat pump is then discussed where after the results are given and the conclusions are drawn.

3. PURE R22 DESIGN METHODOLOGY

The design procedure developed is very tedious. Therefore, in this section the methodology is not discussed in detail, only a concentrated description is given.

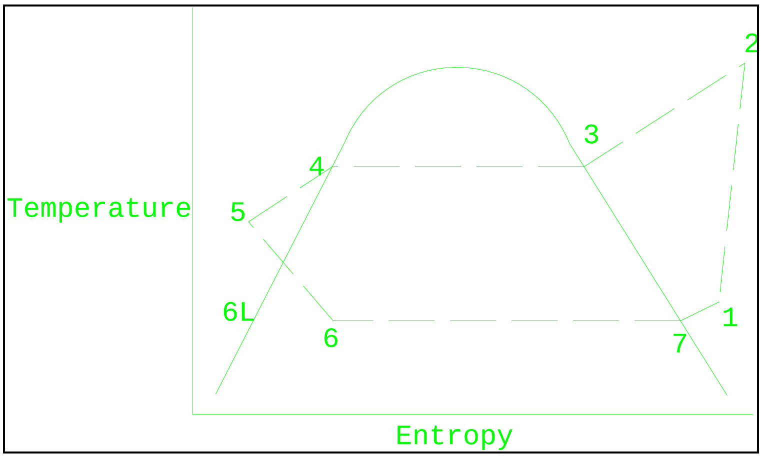

Figure 1. Schematic representation of vapour compression cycle on a temperature entropy diagram with pure refrigerant.

The design of the pure R22 heat pumps starts at point 1 in Figure 1, which is the compressor inlet. The compressor selected is a single cylinder compressor with a displacement rate of 0.0261 l/s and a nominal heating capacity of 4.4 kW at ARI[1] conditions. The compressor manufactures recommend a superheat of 11.11 °C. Thus at a design evaporating temperature of 0 °C and superheat of 11.11 °C, point 1 is known. Using the compressor performance curves, the heat pump capacity, mass flow and compressor power can be obtained, by specifying the condenser and evaporator temperatures (0 °C and 65 °C respectively, for this case.) These temperatures represent the worst case scenario that would give the largest lengths of the evaporator and condenser.

In the case of a hermicaly sealed compressor it is fair to assume that all the input power is transferred to the refrigerant - either in the form of work or heat. Point 2 can be determined since the compressor discharge pressure is known from the design condensing temperature and the enthalpy at point 2 is known from Equation 1.

$$P = m(h_2 - h_1) \qquad (1)$$

The design of the condenser is divided into three regions, namely the superheat region (between points 2 and 3), the two phase region (between points 3 and 4) and the subcooled region (between points 4 and 5). The properties of the refrigerant at the inlet and outlet (points 3 and 4) of the two phase region can be determined from the property chart of R22 at the specified evaporating temperature which is 65 °C, whilst the temperature of the refrigerant at the outlet of the subcooled region (point 5) is 8.3 °C lower than the temperature at point 4. This subcooling temperature is given by the compressor manufacturers for a given cycle for the capacity curves and will be used as the subcooled temperature throughout the text.

If at first the assumption is made that no pressure losses through a region occur, the length of that region may be calculated using Equation 2.

[1] ARI conditions is at an evaporating emperature of 7° C and condensing temperature of 54 °C.

$$L_{io} = Q_{io} / (d_i \ \pi \ U_{io} \ T_{io}) \qquad (2)$$

The heat transfer from the refrigerant to the water is calculated using Equation 3.

$$Q_{io} = m\,(h_i - h_o) \qquad (3)$$

With the water temperature at the condenser outlet specified as 65 °C, the water inlet temperature of a region can be calculated from:

$$Q_{io} = m_w\, C_p\, (T_{wo} - T_{wi}) \qquad (4)$$

With these water temperatures and the refrigerant inlet and outlet temperatures, the logarithmic mean temperature difference is calculated for the three regions. The overall heat transfer coefficient for a region can be obtained from:

$$U_{io} = \{(1/h_r) + (d_i \ln(d_o/d_i)/(2k)) + d_i/(d_o h_w)\}^{-1} \qquad (5)$$

The Petukhov (Holman 1990) equation is used to calculate the convection heat transfer coefficient of the single phase regions of the refrigerant (subcooled and superheat) as well as the water in the annulus, whilst a semi - empirical equation of Fujji (Shizuya, et al 1995) is used for the two phase flow of the refrigerant.

After the length of a section is found, the pressure drop of the refrigerant is calculated. The Halaand (White 1986) equation is used to determine the pressure drop of the single phase regions whilst the method of Jung and Rademacher (1993) is used in the two phase region. The outlet of each region is redefined by subtracting the pressure drop from the pressure at the inlet of that region. With the new thermodynamic properties at the outlet of a region known, the length of that region is recalculated until the pressure drop converges.

The total length of the condenser is the sum of the pipe length of the three regions.

After systematic experimentation with different inner and outer pipe diameters as well as water mass flow rates, it was found that a 9.53 mm outside diameter tube with a total length of 7.93 m gives an acceptable pressure drop for the refrigerant on the inside of a pipe-in-pipe heat exchanger with an outside pipe with outer diameter of 15.88 mm and water mass flow rate of 0.04 kg/s.

Expansion through the expansion valve is assumed to be adiabatic, resulting in the same enthalpy at point 5 and point 6. Point 6 is thus known since the evaporation temperature is defined and the enthalpy at point 6 is known.

The design of the evaporator is divided into two regions, namely the two phase region, and the superheat region. The properties of the refrigerant at the inlet and outlet of the two phase region can be determined from the property chart of R22 whilst the temperature of the refrigerant at the outlet of the superheat region is 11.11 °C higher than the temperature at point 7. This superheated temperature is prescribed by the compressor manufacturers.

Again, if at first the assumption is made that no pressure losses through a region occur, the length of that region is calculated using Equation 2, whilst the heat transfer from the water to the refrigerant is calculated using Equation 3. With the inlet water temperature at the evaporator specified as 16 °C, the water outlet temperature of a region can be calculated using Equation 4. With these water temperatures and the refrigerant inlet and outlet temperatures, the logarithmic mean temperature difference is calculated. The overall heat transfer coefficient can be obtained from Equation 5.

Again, just as for the condenser, the Petukhov (Holman 1990) equation is used to calculate the convection heat transfer coefficient of the single phase regions of the refrigerant (subcooled and super heat) as well as the water in the annulus, but now for the evaporator an equation of Jung and Radermacher (1993) is used for the two phase flow of the refrigerant.

After the length of a section is found, the pressure drop of the refrigerant is calculated. The Halaand (White 1986) equation is used to determine the pressure drop of the single phase regions whilst the method of Jung and Rademacher (1993) is used in the two phase region. The outlet of each region is redefined by subtracting the pressure drop from the pressure at the inlet of that region. With the new thermodynamic properties at the outlet of a region known, the length of that region is recalculated until the pressure drop converge.

The total length of the evaporator is the sum of the pipe length of the three regions.

After systematic experimentation with different inner and outer pipe diameters as well as water mass flow rates, it was found that a 25.4 mm outside diameter tube with a total length of 4.89 m gives an acceptable pressure drop for the refrigerant on the inside of a pipe-in-pipe heat exchanger with an outside pipe diameter of 15.88 mm and water mass flow rate of 0.4 kg/s.

For verification and comparison purposes the performance of the geometry calculated above was also simulated with HPSIM, a computer program (Greyvenstein 1988). These results as well as the difference between the calculated and numerically predicted values are summarised in Table 1. It can be concluded that in general a good agreement exists between the calculated and numerically predicted values, even though the same equations were not used in the prediction of the heat transfer coefficients. For more detail on the calculation of the convection coefficients in HPSIM the interested reader is referred to Greyvenstein (1988).

Property	Calculated	HPSIM (numerically predicted)	Absolute difference[%]
Compressor power	1 679 W	1 734 W	3.2
Refrigerant mass flow	0.01512 kg/s	0.01744 kg/s	13.3
Heating capacity	3 841 W	4 228 W	9.2
Cooling capacity	2 160 W	2 494 W	13.4
Heating COP	2.28	2.43	6.1
Water pump power	8.3 W	8.2 W	1.2
Condenser water pressure drop	7.75 kPa	7.55 kPa	2.7
Evaporator water pressure drop	19.9 kPa	20.7 kPa	3.9
T_1	11.07 °C	12.73 °C	0.6
T_2	175.2 °C	161.5 °C	3.1
T_3	65.49 °C	62.18 °C	0.99
T_4	65.36 °C	62.05 °C	0.99
T_5	57.03 °C	55.53 °C	0.46
T_6	0 °C	1.71 °C	0.62
T_7	-0.04 °C	1.62 °C	0.60
p_1	497.1 kPa	523.2 kPa	4.99
p_2	2 738 kPa	2 551 kPa	7.34
p_3	2 734 kPa	2 545 kPa	7.45
p_4	2 727 kPa	2 538 kPa	7.46
p_5	2 727 kPa	2 538 kPa	7.45
p_6	497.7 kPa	525.7 kPa	5.33
p_7	497.1 kPa	524 kPa	5.13

Table 1. Comparison between calculated and numerically predicted values.

4. NON - AZEOTROPIC DESIGN METHODOLOGY

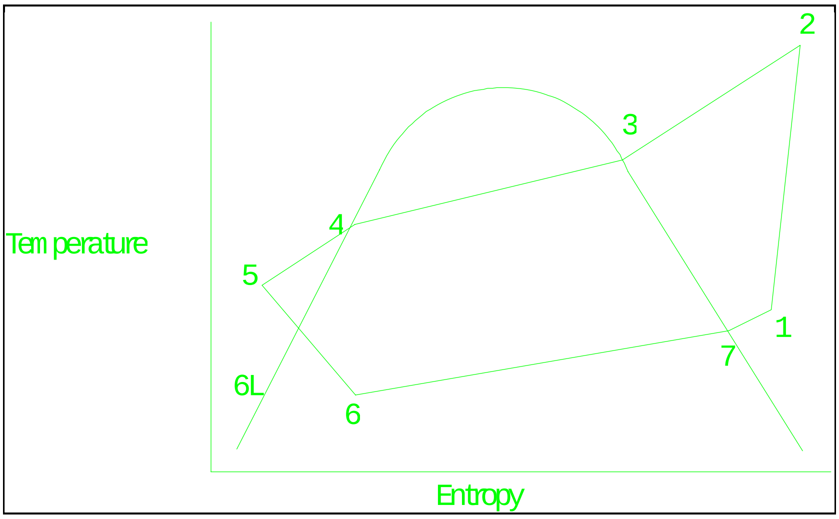

Figure 2. Schematic representation of the vapor compression cycle on a temperature entropy diagram with a non-azeotropic refrigerant mixture.

With the design of the non - azeotropic refrigerant heat pump, the only difference is in the estimation of the enthalpy difference of the compressor. Since no R142b compressors are available on the market, the same compressor is selected for the design of the non - azeotropic refrigerant heat pump as for the R22 heat pump design. Furthermore is R142b compatible with the existing hardware and lubricants of R22 compressors (Johannsen 1992). Unfortunately new performance curves valid for a non - azeotropic refrigerant mixture had to be estimated by using the R22 as input data, since the compressor performance curves are only valid for pure R22.

These estimations are based on the mass flow rate which is proportional to the inlet density of the refrigerant, the volumetric efficiency and the displacement rate of the compressor. In equation form:

$$m_r = \rho_r \, \eta_v \, V \qquad (6)$$

By rearranging the terms in Equation 6 so that the volumetric efficiency is the subject and by assuming the volumetric efficiency for a non-azeotropic refrigerant mixture and a pure refrigerant are equal at the same pressure ratio it follows that:

$$\eta_v = m_r / \rho_r V = m_m / \rho_m V \qquad (7)$$

from where the mass flow rate of the mixture can be solved at the same pressure ratio:

$$m_m = m_r \, \rho_m / \rho_r \qquad (8)$$

The mixture mass flow as well as the compressor power are needed when a non-azeotropic mixture is used in the place of R22. The compressor power as function of isentropic enthalpy change during compression and isentropic efficiency is given by:

$$P_r = (h_{2sr} - h_{1r})\, m_r / \eta_s \qquad (9)$$

Assuming that the isentropic efficiency of a non-azeotropic refrigerant mixture and a pure refrigerant are equal at the same pressure ratio over the compressor, it follows that:

$$\eta_s = (h_{2sr} - h_{1r})\, m_r / P_r = (h_{2sm} - h_{1m})\, m_m / P_m \qquad (10)$$

Therefore the compressor power for the mixture can be estimated, at the same pressure ratio as the pure refrigerant, using the following equation.

$$P_m = (h_{2sm} - h_{1m})\, m_m\, P_r / \{(h_{2sr} - h_{1r})\, m_r\} \qquad (11)$$

The REFPROP (Gallagher 1993) computer programme was used for the calculation of pure and non-azeotropic refrigerant properties. Using the compressor curves for R22 together with Equations 8 and 11, the mass flow and compressor power were determined as a function of different evaporating and condensing pressures for different non-azeotropic concentrations. An example of these results for a concentration of 60% R22 and 40% R142b is shown in Figure 3. Performance data is usually expressed as a function of condensing and evaporating temperatures, this is impossible when working with non-azeotropic refrigerants due to the temperature glides during the evaporation and condensation processes. Therefore, in this study performance data is expressed as a function of evaporating and condensing pressures.

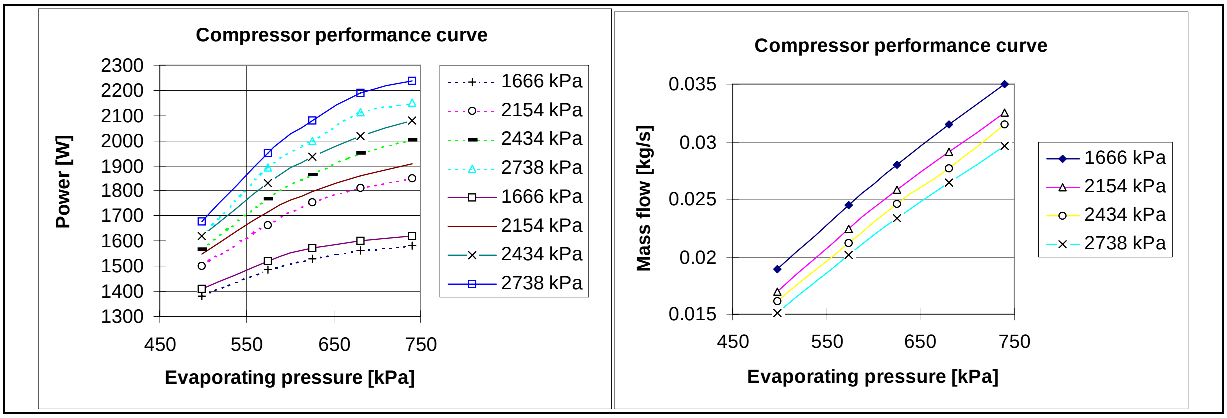

Figure 3. A comparison of R22 mass flow and compressor power data as supplied by the compressor manufacturer plotted against estimated non-azeotropic mixture of 60% R22 and 40% R142b. The solid line is for R22 and the dotted line is for the mixture. The pressures in the legend are the condensing pressure.

It may be observed from Figure 3 that there is a decrease in compressor power whilst the mass flow stays relatively constant (the lines are on top of each other) at the same condensing and evaporating pressures for the non-azeotropic mixture.

Using compressor curves similar to Figure 3 for different concentrations of R22 and R142b to obtain new mass flows and compressor powers, the same design procedure is followed as explained previously for the R22 heat pump.

5. COMPARISON METHOD

A popular method (Högberg *et al* 1992, Johannsen 1992) used in research studies to compare pure refrigerant mixtures with refrigerant mixtures is the comparison between the Carnot - and Lorentz cycles. In this method the dew point temperature in the condenser (Figure 2 point 3) and the bubble point temperature in the evaporator (Figure 2 point 6) are kept the same for the two cycles. These two temperatures are influenced by the temperatures of the heat sink and heat source.

In most heat pump applications the heat source is water or air at atmospheric conditions in the region of 20 °C. If a maximum temperature glide of 7 °C is assumed for the mixture and a superheat of 11.11 °C (a recommended value provided by the compressor manufacturer) an adequate average evaporating temperature would be in the region of 0 °C.

Unfortunately, at this low temperature the pressure of R142b is also very low. The gas that is trapped in the clearance volume of the compressor must expand to a pressure low enough for the suction valves to open and draw more gas in. If the pressure at the inlet of the compressor is too low (as in this case) no gas would be sucked into the compressor and the mass flow of the refrigerant would be zero. To assure a mass flow of 0.00126 kg/s which is only 3% of the maximum mass flow of the selected compressor, the suction pressure must be higher than 321 kPa. At this pressure it can be observed from Figure 4 that as the concentration of R142b is increased, the evaporating temperature increases, resulting in higher heat source temperatures needed.

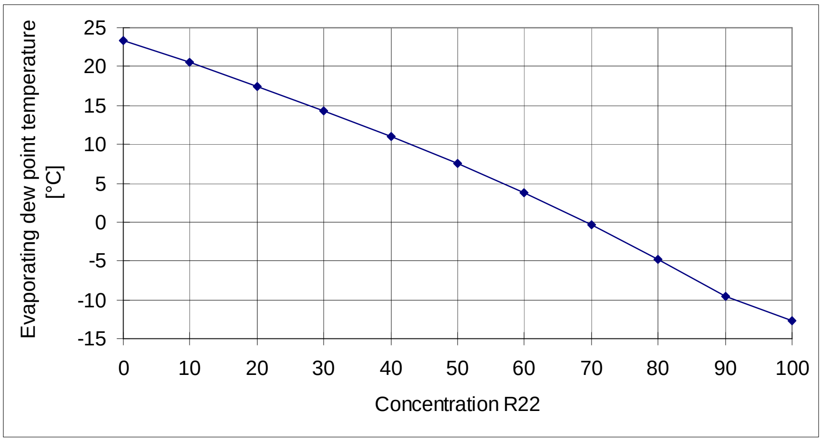

Figure 4. Evaporator dew point temperature of a mixture of R22 and R142b at different concentrations and a pressure of 321 kPa.

Although the heat source temperature is excessively high for a case where 100% R142b is used as refrigerant, the restriction to this temperature is due to the practical limitations of the selected compressor. In this study the heat source temperature will be chosen high to compensate for the low pressure in the compressor, but for practical applications a compressor with a high pressure ratio and low suction pressure would be better suited. At the time of this study such a compressor was not available but the results will still show the same tendency as in the case with low heat source temperatures. Therefore for the purposes of this study a dew point temperature in the condenser of 65 °C and a bubble point temperature in the evaporator of 25 °C is used.

6. RESULTS AND DISCUSSION

Evaluating the results presented in Figures 5 to 18, it follows that the length of the condenser increases, as can be deduced in Figure 5, as the percentage of R22 is reduced. At first the increase is nearly linear, but as the concentration of R22 is decreased (approximately 40% R22), the length increases more substantially. Whilst the condenser length increases with addition of R142b, the length of the evaporator, also increases but reaches a maximum at 50% R22 where after it decreases.

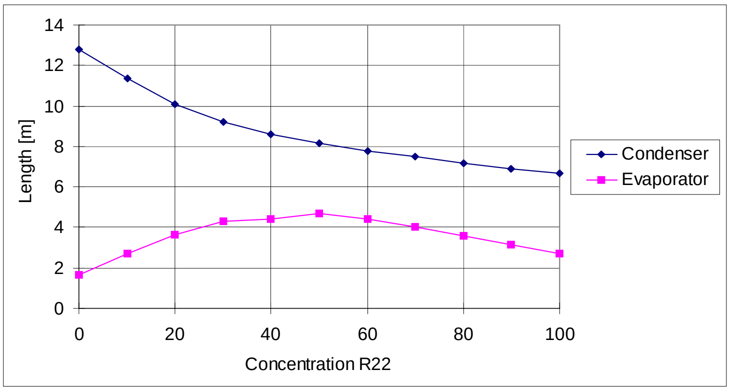

Figure 5. Lengths of condenser and evaporator.

The compressor discharge temperature (T_2) decreases slightly until the concentration of R22 is 20% where after it increases sharply with any further addition of R142b (as can be concluded from Figure 6.) The danger of the decomposition of the lubrication oil is therefore a factor at high concentrations of R142b. The other refrigerant temperatures (T_1, T_3, T_4, T_5, T_6 and T_7) will be discussed later.

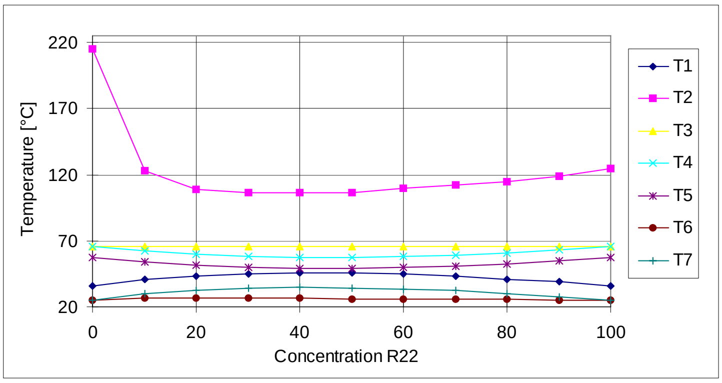

Figure 6. Temperature at different stations.

The water outlet temperature in the condenser is kept constant at 65 °C. This is part of the boundary conditions in the condenser as shown in Figure 7. It can be seen that for high concentrations of R22 (more than 60%) the water inlet temperature stays nearly constant, but at lower concentrations (less than 60% R22) the water inlet temperature must be increased to deliver the desired outlet water temperature. In the evaporator (Figure 8) the water inlet temperature was kept constant at 50 °C. Again this is part of the boundary conditions in the evaporator. The same tendency can be observed in this figure for the evaporator as in the case of the condenser, namely that at concentrations higher than 50% R22, the water outlet temperature is nearly constant, but at lower concentrations the water outlet temperature is increasing. The reason why the condenser inlet temperature and evaporator outlet temperature increase, is that the heating capacity decreases with high concentrations of R142b this will be discussed later.

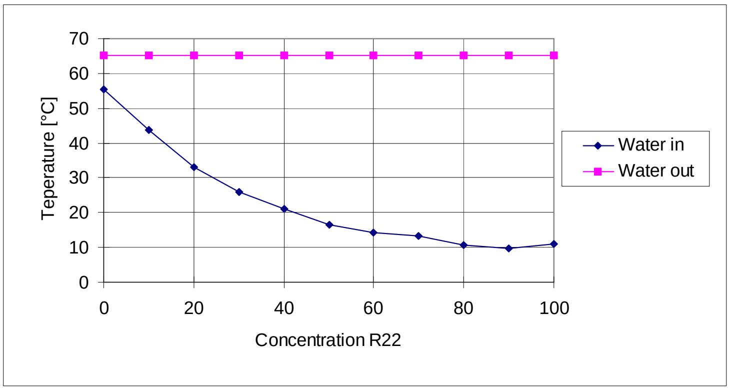

Figure 7. Condenser water inlet and outlet temperatures.

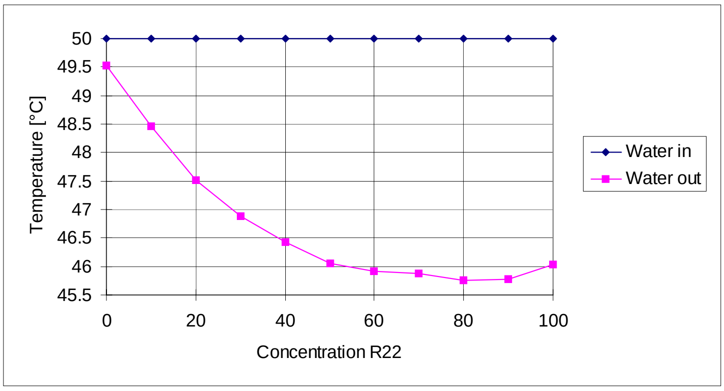

Figure 8. Evaporator water inlet and outlet temperatures.

From Figure 9 it can be deduced that the convection heat transfer coefficients are reducing with an increase in the amount of R142b. At the same time the refrigerant mass flow (m_m) is decreasing with approximately 89% as shown in Figure 10. The reason for this is the combination of the reduction in the mass flow of a pure R22 heat pump (m_r) and inlet density of the mixture (ρ_m) in Equation 8 as shown in Figure 11.

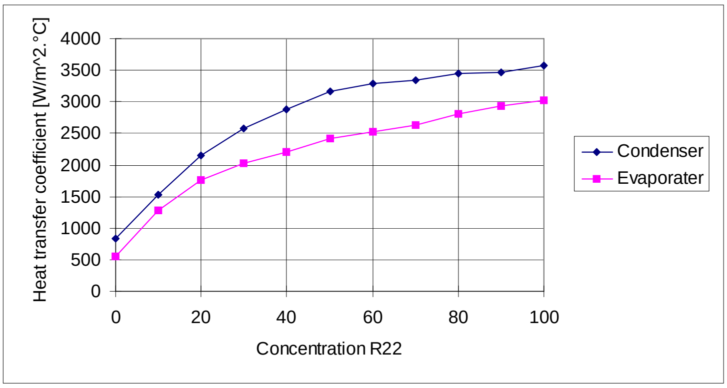

Figure 9. Convection heat transfer coefficient during evaporation and condensation.

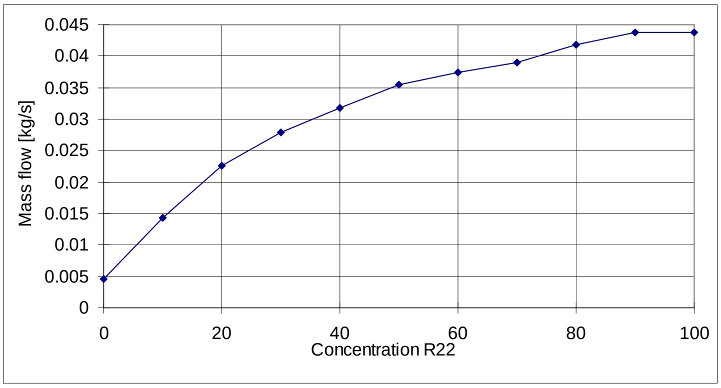

Figure 10. Refrigerant mass flow.

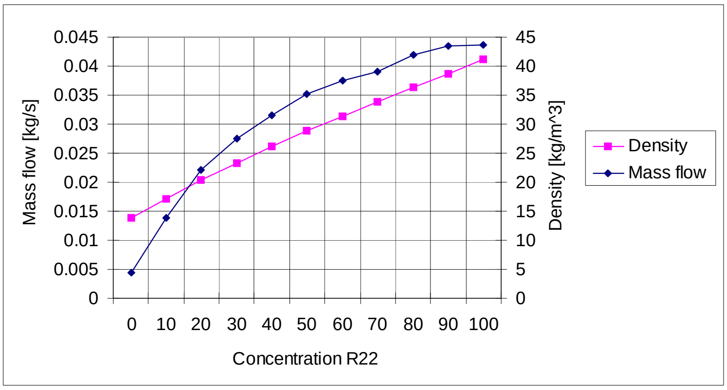

Figure 11. Density of refrigerant mixture at compressor inlet and mass flow of pure R22 from performance curves at the same pressure as the mixture.

As the concentration of R22 is reduced in the mixture, the compressor input power decreases as shown in Figure 12. This reduction in inlet power results in energy savings as well as a reduction in electrical cost. The reason for the reduction in inlet power being mainly the reduction in mass flow of the refrigerant (m_m) as already discussed in Figure 10. Furthermore, the enthalpy difference decreases with an increased concentration of R142b which may be attributed especially to the lowering average temperature difference between the condenser and evaporator (Figure 13). At concentrations less than 20% R22 the average temperature difference between the condenser and evaporator increases substantially. This increase does not increase the compressor input power since the refrigerant mass flow decreases substantially at these low concentrations of R22 as was discussed earlier.

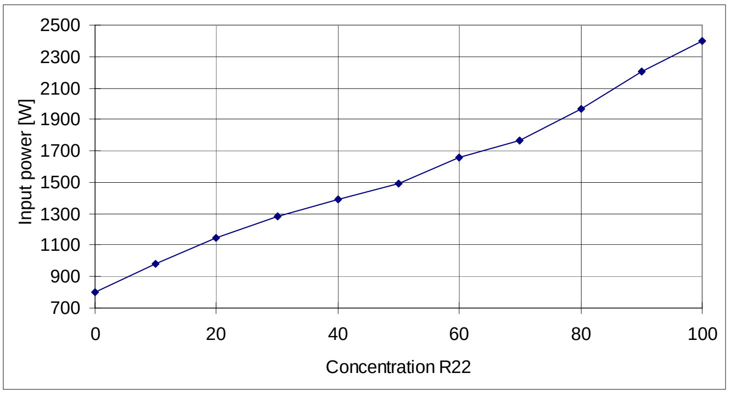

Figure 12. Input compressor power.

Since the dew point temperature (T_3) in the condenser is kept constant, the bubble point temperature (T_4) and condenser outlet temperature (T_5) initially decrease as the concentration of R22 is reduced. This was already shown in Figure 6. The reason for this is due to temperature glides that increase as the concentration of R142b is increased. A minimum condenser outlet temperature (T_5) value is reached at approximately 50% R142b, resulting in a lower average temperature in the condenser as shown in Figure 13. As the temperature glides reduce (Figure 6) these temperatures increase with an enrichment of R142b and consequently increases the average temperature in the condenser. By keeping the bubble point temperature (T_6) in the evaporator constant, the dew point temperature (T_7) and evaporator outlet temperatures (T_1) increase due to temperature glides with an enrichment of R142b in the mixture, and reach a maximum at 50% R142b resulting in an increase in the average evaporator temperature (Figure 13). Further enrichment of R142b leads to a reduction in these temperatures. The difference between the average condenser - and average evaporator temperatures is also shown in Figure 13.

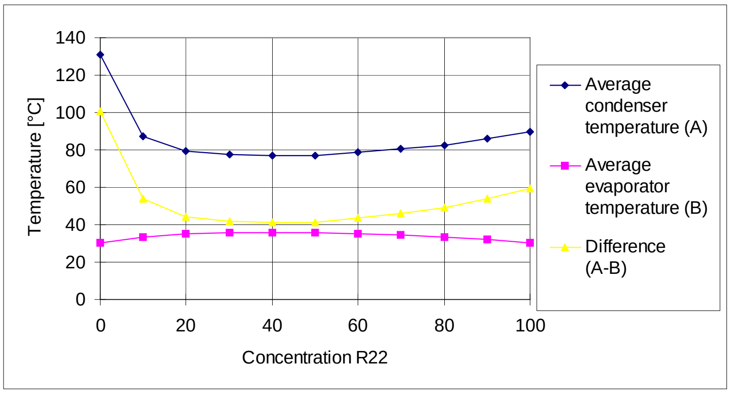

Figure 13. Average refrigerant temperatures in condenser and evaporator as well as the temperature difference.

Figure 14 shows the logarithmic mean temperature difference of the refrigerant and water for the condenser and evaporator. This value decreases in the condenser as the amount of R142b is increased. A minimum value in the evaporator is reached at a concentration of 50% R22. Since the logarithmic mean temperature difference is used to calculate the length of the heat exchangers (Equation 2) it can be concluded from Figure 14 that the tendency of the logarithmic mean temperature difference is responsible for the length of the heat exchangers in Figure 5.

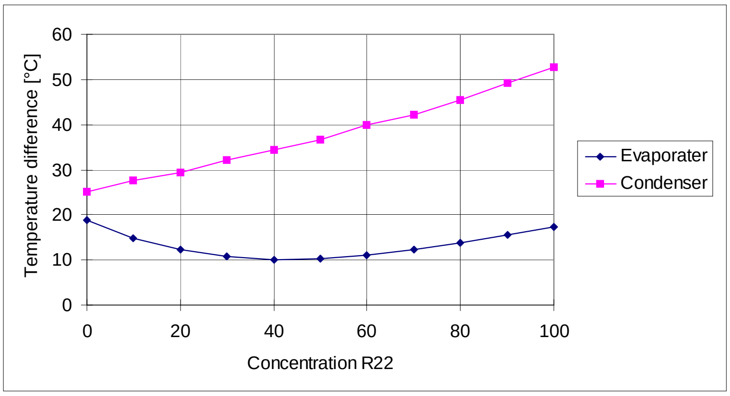

Figure 14. The logarithmic mean temperature difference between the refrigerant and water in the evaporator and condenser.

The cooling and heating capacities are given in Figures 15 and 16. In both cases the maximum capacities occur at a mixture of approximately 90% R22 and 10% R142b after which it reduces monotonically with the enrichment of R142b. The lowest capacity is at 100% R142b. The reason is the reduction in mass flow as already shown in Figure 10.

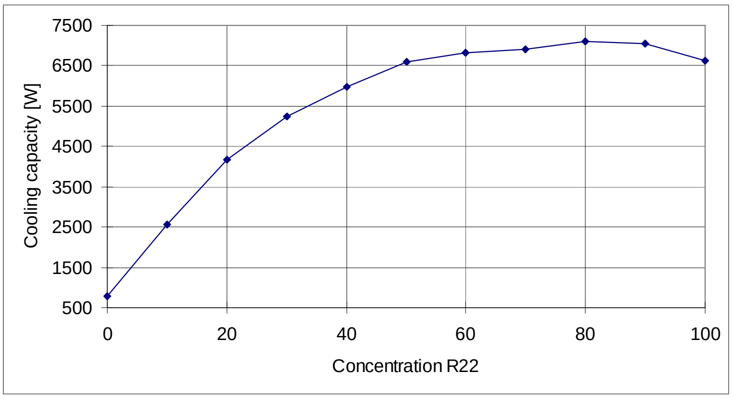

Figure 15. Cooling capacity.

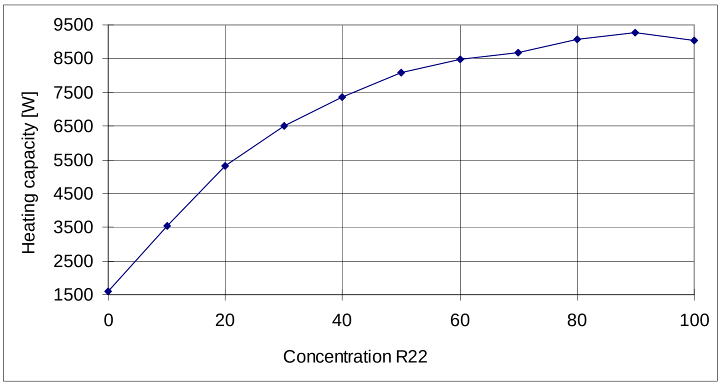

Figure 16. Heating capacity.

As the concentration of the R142b increases the compressor power is reduced (Figure 12). One expects this to lead to an increase in the COP, but since R142b is a low capacity refrigerant, the heating capacity (Figure 16) is reduced with an increase of R142b. At first the reduction in compressor power is higher than the reduction in heating capacity up to a concentration of 50% R22, leading to an increase in COP as shown in Figure 17. At concentrations less than 50% R22 the reduction in heating capacity is higher than the reduction in compressor power, leading to a decrease in COP. It is also evident from this figure that the Lorentz COP follows the same tendency as the calculated COP.

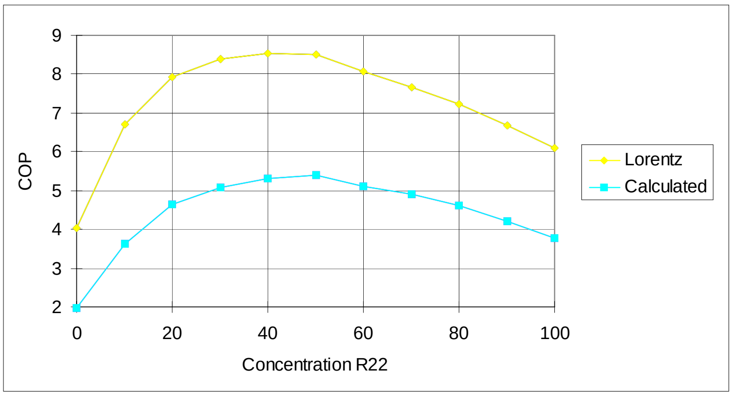

Figure 17. Comparison between the heating COPs for different cycles.

Figure 18 shows the pressure ratio over the compressor. A minimum pressure ratio occurs at a concentration of 50% R22 and 50% R142b. A lowering of the compressor pressure ratio leads to reduced load on the crank shaft and bearings thus increasing the compressors life.

From a theoretical view point it therefore seems that a non-azeotropic mixture of R22 and R142b can be used to increase the compressors life, coefficient of performance and heating capacity of R22 hot water heat pumps. The optimum point is difficult to define since in certain applications one variable may be more important than the other.

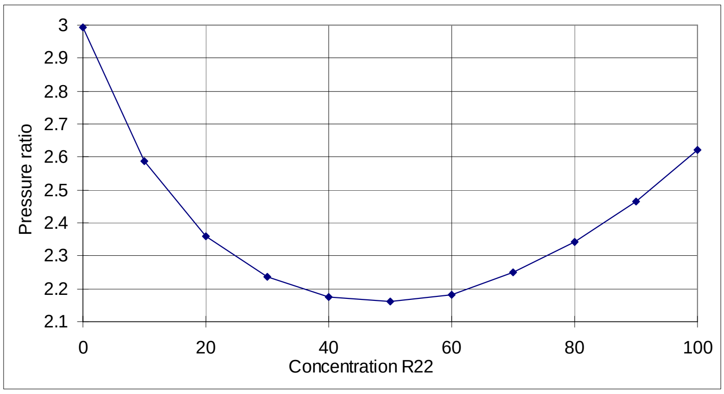

Figure 18. Pressure ratio of compressor.

7. CONCLUSIONS

Due to a decrease in refrigerant mass flow and a decrease in enthalpy difference of the refrigerant in the heat exchangers, the heating and cooling capacities decrease substantially with a decrease in R22 in the mixture. With this decrease in capacity the temperature difference of the water in the heat exchangers also decreases, resulting in lower logarithmic mean temperature differences in the condenser and higher logarithmic mean temperature differences in the evaporator. Considering that the heat transfer coefficients also decrease, it follows that the length of the condenser must increase. The length of the evaporator increases up to a concentration of 50% R22. At lower concentrations of R22 the effect of lower cooling capacity and increasing logarithmic mean temperature difference results in a decrease in evaporator length.

Except for the reduction of the evaporator length, other advantages may be identified upon comparison of a non - azeotropic refrigerant mixture and a pure refrigerant: Firstly, the coefficient of performance increased with 44% at a concentration of 50% R22. This means that nearly twice as much heating can be done with a non - azeotropic refrigerant mixture with the same amount of compressor input power as a pure R22 heat pump. Secondly, the heating capacity can be increased by 2.5% if a concentration of 90% R22 and 10% R142b is used. Thirdly, the pressure ratio over the compressor reduces with 18% at a concentration of 50% R22. This would lead to longer compressor life. Frothily, as the compressor input power is reduced, energy is saved and the cost of electricity reduced.

These theoretical results show the influence of a non - azeotropic refrigerant on the performance of a hot water heat pump and experimental verification would be suggested.

8. REFERENCES

Basson J A (1983*), "Die verwarming van huishoudelike water",* National Building Research Institute, Internal report, CSIR, Pretoria.

Gallagher J, McLinden M, Morrison G, and Huber M (1993), *"NIST thermodynamic properties of refrigerants and refrigerant mixtures"*, (REFPROP), U.S. Department of Commerce, Version 4, November, 1993.

Greyvenstein G P (1988), *"A computer simulation model for the design and optimization of heat pumps and refrigeration systems*", South African Journal of Science, Vol. 84, June, pp. 494-502.

Högberg M, Vamling L, and Berntsson T (1992), *"Calculation methods for comparing the performance of pure and mixed working fluids in heat pump applications"*, International Journal of Refrigeration, Vol. 16, No. 6, pp. 403-412.

Holman J P (1990), *"Heat transfer"*, New York, Mc Graw Hill, p.285.

Johannsen A F B (1992), *"Potential of non-azeotropic refrigerant mixtures for water-heating heat pumps in South Africa"*, Energy Branch, Department of Mineral and Energy Affairs, South Africa, Report number ED 8807.

Johannsen A and Kaiser G (1986), *"Potential of electrically operated heat pumps for heating water in South Africa"*, CSIR, Report number 615, Pretoria, August.

Jung D S and Radermacher R (1993), *"Prediction of evaporation heat transfer coefficient and pressure drop of refrigerant mixtures in horizontal tubes"*, International Journal of Refrigeration, Vol. 16, No. 3, pp. 201-208.

Meyer J P and Greyvenstein G P (1992), *"Hot water for large residential units, hospitals and laundries with heat pumps in South Africa: A techno - economic analysis"*, Energy Conversion and Management, Vol. 33, No. 2, pp. 135 - 143.

Salas C E and Marianne (1992), *"Guide to refrigeration CFC 's"*, Fairmont Press, Lilburn, pp. 107 - 108.

Shizuya M, Itoh M, and Hijikata K (1995), *"Condensation of non - azeotropic binary refrigerant mixtures including R22 as a more volatile component inside a horizontal tube"*, Journal of Heat Transfer, Vol. 117, May, pp. 538-543.

Walker R N (1993), *"Applying industrial heat pumps"*, Plant Engineering, Vol. 23, September, pp. 65 - 67.

White F M (1986), *"Fluid mechanics"*, New York, McGraw Hill, p. 314.